Published in final edited form as:
Neuropharmacology. 2013 March ; 66: 122–132. doi:10.1016/j.neuropharm.2012.03.003.

Functional selectivity induced by $mGlu_4$ receptor positive allosteric modulation and concomitant activation of G_q coupled receptors

Shen Yin, **Rocio Zamorano**, **P. Jeffrey Conn**, and **Colleen M. Niswender***
Vanderbilt Center for Neuroscience Drug Discovery, Department of Pharmacology, Vanderbilt University Medical Center, Nashville, TN 37232, USA

Abstract

Metabotropic glutamate receptors (mGlus) are a group of Family C Seven Transmembrane Spanning Receptors (7TMRs) that play important roles in modulating signaling transduction, particularly within the central nervous system. $mGlu_4$ belongs to a subfamily of mGlus that is predominantly coupled to $G_{i/o}$ G proteins. We now report that the ubiquitous autacoid and neuromodulator, histamine, induces substantial glutamate-activated calcium mobilization in $mGlu_4$-expressing cells, an effect which is observed in the absence of co-expressed chimeric G proteins. This strong induction of calcium signaling downstream of glutamate activation of $mGlu_4$ depends upon the presence of H_1 histamine receptors. Interestingly, the potentiating effect of histamine activation does not extend to other $mGlu_4$-mediated signaling events downstream of $G_{i/o}$ G proteins, such as cAMP inhibition, suggesting that the presence of G_q coupled receptors such as H_1 may bias normal $mGlu_4$-mediated $G_{i/o}$ signaling events. When the activity induced by small molecule positive allosteric modulators of $mGlu_4$ is assessed, the potentiated signaling of $mGlu_4$ is further biased by histamine toward calcium-dependent pathways. These results suggest that $G_{i/o}$-coupled mGlus may induce substantial, and potentially unexpected, calcium-mediated signaling events if stimulation occurs concomitantly with activation of G_q receptors. Additionally, our results suggest that signaling induced by small molecule positive allosteric modulators may be substantially biased when G_q receptors are co-activated.

This article is part of a Special Issue entitled ‘mGluR’

Keywords

Glutamate; Histamine; Receptor; Allosteric modulator; Functional selectivity

1. Introduction

Seven Transmembrane Spanning/G-Protein-Coupled Receptors (7TMRs/GPCRs) represent the majority of drug targets currently used in clinical practice. Much interest has recently been placed on the discovery and characterization of allosteric modulators for these receptors due to several potential advantages over traditional orthosteric ligands in terms of drug development (reviewed in(Keov et al., 2011)). For example, many natural endogenous ligands are peptides or small amino acids which possess limitations in pharmacokinetic

*Corresponding author. Tel.: +1 615 343 4303; fax: +1 615 322 8577. Colleen.niswender@vanderbilt.edu (C.M. Niswender).

Appendix. Supplementary material
Supplementary material associated with this article can be found, in the online version, at doi:10.1016/j.neuropharm.2012.03.003.

properties, preventing their development as drug candidates. Additionally, the orthosteric agonist binding sites of many 7TMRs are highly conserved across family members, making selectivity for a particular receptor within one group difficult to achieve. Due to their interaction with the receptor at a site distinct from the orthosteric site, allosteric ligands often possess very high receptor selectivity. Allosteric modulators also have the ability to provide a more subtle and physiologically-relevant approach to increasing or decreasing target activity because receptor regulation will occur only in the presence of the endogenous ligand (Bridges and Lindsley, 2008; Conn et al., 2009). Furthermore, allosteric potentiators, or positive allosteric modulators (PAMs), may, in some cases, avoid receptor desensitization and/or downregulation that can occur after chronic administration of an orthosteric agonist (Bridges and Lindsley, 2008; Conn et al., 2009). As allosteric modulators function by exerting either positive (PAMs) or negative (NAMs) cooperativity with the orthosteric ligand, mechanistically they will exhibit a “ceiling” effect (i.e., maximal receptor occupancy may not translate to maximal effect on receptor activation), which may avoid target/mechanism-mediated side effects that could arise from accidental overdose.

While allosteric modulators of 7TMRs provide potential advantages/distinctions over orthosteric ligands, these compounds also greatly complicate our understanding of receptor pharmacology. In recent years, there has been a growing appreciation of the ability of a single 7TMR to simultaneously regulate multiple signaling cascades (Kenakin, 2005), some of which are G protein-independent, such as β arrestin-regulated pathways. This phenomenon, now well established for orthosteric ligands, has been termed “functional selectivity”, “biased signaling”, or “ligand directed trafficking” (Urban et al., 2007; Keov et al., 2011); we will refer to this phenomenon as functional selectivity in the present manuscript. There are now also clear examples of 7TMR allosteric modulator-mediated functional selectivity (Mathiesen et al., 2005; Marlo et al., 2009). While this behavior introduces complexity into ligand development, it is anticipated that capitalizing on functionally selective effects will provide exciting opportunities to tailor new drug therapy to specifically regulate coupling of 7TMRs to beneficial signaling pathways but not others, potentially reducing adverse effects.

There are numerous mechanisms by which functionally selective pharmacology can be induced by allosteric ligands. For example, 7TMRs have the ability to adopt multiple structural conformations, any of which might be stabilized by an allosteric modulator. This can translate into the ability of a modulator to preferentially regulate some pathways and not others based on the particular conformation they stabilize. Receptor activity is also regulated by other cellular proteins, such as G proteins, arrestins, or scaffolding proteins, which also act in an allosteric fashion to affect receptor conformations. In this case, compound pharmacology can be altered depending on the context in which a receptor is expressed (e.g., (Niswender et al., 2010)), presumably due to the different proteins or cellular components interacting with the receptor in various cell types.

An alternate possibility that may affect the outcome of functional selectivity would be convergent signaling pathways that are activated (or inhibited, or simply absent) in a certain temporal or spatial context. It has previously been demonstrated that activation of the $G_{i/o}$-coupled $GABA_B$ receptor, in conjunction with the G_q-coupled metabotropic glutamate 1 ($mGlu_1$) receptor, produces a signaling convergence at the level of phospholipase C β3 ($PLC_{\beta 3}$) to induce potentiated calcium mobilization (Pin et al., 2009; Rives et al., 2009). In these studies, this phenomenon was not due to heterodimerization/oligomerization of the receptors, was generalizable to other receptor pairs, and was demonstrated to exhibit functional relevance in cerebellar Purkinje cells and cultured cortical neurons where these two receptors are co-expressed (Rives et al., 2009). In the present manuscript, we extend these findings to explore potentially functionally selective effects induced by this type of

signaling convergence. We describe that, as for the $GABA_B$ and $mGlu_1$ receptor combination, activation of a G_q coupled histamine receptor, the H_1 receptor, dramatically potentiates the ability of the $G_{i/o}$-coupled metabotropic glutamate 4 ($mGlu_4$) receptor to induce intracellular calcium mobilization. However, histamine does not potentiate the ability of $mGlu_4$ activation to modulate other "common" $G_{i/o}$-regulated signaling cascades, such as cAMP inhibition. These results suggest that H_1 co-activation biases $mGlu_4$-mediated signaling events toward certain signaling pathways. Furthermore, when small molecule PAMs of $mGlu_4$, are included in these assays, the potentiated signaling of $mGlu_4$ is further biased by histamine toward calcium-dependent pathways. Our results suggest that convergence of these signaling pathways may result in substantial, and potentially unexpected, increases in calcium responses downstream of $mGlu_4$ activation, particularly when receptor activity is potentiated using positive allosteric modulators.

2. Materials and methods

2.1. Cell line establishment and cell culture

Establishment and culture of the human $mGlu_4$ ($hmGlu_4$)/G_{qi5}/CHO-DHFR(−) has been described in (Niswender et al., 2008). All cell culture reagents were purchased from Invitrogen (Carlsbad, CA) unless otherwise noted.

Guinea pig H_1 (gp H_1)/CHO-K1 cells were obtained by stable transfection of CHO-K1 cells with guinea pig H_1 receptor in pcDNA3.1 vector (a generous gift of Mike Zhu, Ohio State University). Single G418-resistant clones were isolated and screened for H_1-mediated calcium mobilization as described below. Monoclonal gpH_1/CHO-K1 cells were cultured in 90% Dulbecco's modified Eagle's medium (DMEM), 10% dialyzed fetal bovine serum (FBS), 100 U/mL penicillin/streptomycin, 20 mM HEPES, 1 mM sodium pyruvate, 2 mM L-glutamine, 20 μg/mL proline (Sigma-Aldrich, Inc., St. Louis, MO) and 400 μg/mL G418 sulfate (Mediatech, Inc., Herndon, VA).

Rat $mGlu_4$/CHO-K1 cells, rat $mGlu_2$/CHO-K1 cells, rat $mGlu_4/H_1$/CHO-K1 cells, and rat $mGlu_2/H_1$/CHO-K1 cells were obtained by stable transfection of either CHO-K1 cells or gpH_1/CHO-K1 cells with rat $mGlu_4$ or $mGlu_2$ receptor in a pIRESpuro3 vector (Invitrogen). Polyclonal cells were cultured in 90% DMEM, 10% dialyzed FBS, 100 U/mL penicillin/streptomycin, 20 mM HEPES, 1 mM sodium pyruvate, 2 mM L-glutamine, 20 μg/mL proline (Sigma-Aldrich, Inc., St. Louis, MO), 20 μg/mL puromycin (Sigma-Aldrich, Inc., St. Louis, MO) without or with 400 μg/mL G418 sulfate (for H_1 expressing cell lines, Mediatech, Inc., Herndon, VA).

Rat $mGlu_4/M_1$/CHO-K1 cells were generated by stable transfection of rat $mGlu_4$/CHO-K1 cells with rat M_1 muscarinic receptor DNA in pcDNA3.1 vector. Polyclonal cells were cultured in 90% DMEM, 10% dialyzed FBS, 100 U/mL penicillin/streptomycin, 20 mM HEPES, 1 mM sodium pyruvate, 2 mM L-glutamine, 20 μg/mL proline (Sigma-Aldrich, Inc., St. Louis, MO), 400 μg/mL G418 sulfate (Mediatech, Inc., Herndon, VA) and 20 μg/mL puromycin (Sigma-Aldrich, Inc., St. Louis, MO).

2.2. Calcium mobilization assays

For assays performed using the Flexstation (Molecular Devices, Sunnyvale, CA), cells were seeded at a density of 60,000 cells/100 μL/well in Costar 96-well tissue culture-treated plates. For assays performed using the Hamamatsu FDSS 6000 or 7000 (Hamamatsu, Japan), cells were seeded at 30,000 cells/20 μL/well in Greiner 384-well clear-bottomed, tissue culture–treated plates. Cells were incubated in assay medium (90% DMEM, 10% dialyzed FBS, 20 mM HEPES and 1 mM sodium pyruvate) overnight at 37 °C/5% CO_2 and assayed the following day.

Fluo-4/acetoxymethyl ester (Invitrogen) was dissolved as a 2.3 mM stock in DMSO and mixed in a 1:1 ratio with 10% (w/v) Pluronic acid F-127 and diluted in assay buffer (Hanks' balanced salt solution, 20 mM HEPES, and 2.5 mM probenecid; Sigma-Aldrich) to a final concentration of 2 μM. Cells were dye-loaded for 45 min at 37 °C; dye was then removed and replaced by appropriate volume of assay buffer. For single-add experiments, a series of different concentrations of glutamate or histamine were diluted into assay buffer as 2× stock. For histamine fold-shift and potency experiments, histamine was diluted as 2× stock and added at the first add. After 150 s, the appropriate volume of a 5× glutamate stock was added in a second addition. For experiments using antagonists or PAMs, compounds were added at a 2× final concentration in the first addition followed by the desired concentration of agonist in the second addition.

2.3. Total RNA isolation, reverse transcription and polymerase chain reaction (RT–PCR)

CHO-K1 cells and $mGlu_4/G_{qi5}$/CHO-DHFR(−) cells were seeded in 10 cm cell culture dishes one day before the experiment. On the second day, cells were harvested and total mRNA from each cell line was extracted using an RNeasy Mini Kit (Qiagen, Valencia, CA). Total RNA was quantified by Nanodrop and 0.5 ug was reversely transcribed into cDNA by iScript cDNA Synthesis Kit (Bio-Rad, Philadelphia PA) according to the manufacturer's protocol. Reactions were carried out both in the presence and in the absence of reverse transcriptase (as negative controls). One tenth of each yielded cDNA sample was used to perform polymerase chain reaction (PCR) using primers for histamine H_1 receptor, which were designed to match the conserved sequence for human, rat and mouse H_1:

H_1 Forward: CTCAACCTGCTGGTGCTGTA

H_1 Reverse: GAAGTCTGTCTCACACTTGTC

pcDNA3.1-gpH_1 (guinea pig H_1 receptor) plasmid was used as positive controls for H_1, while water was used as a negative control for PCR reactions. The amplification protocol was 95 °C for 2 min, 30 cycles of 95 °C for 30 s, 58 °C for 30 s, and 72 °C for 1.5 min. The final extension step was at 72 °C for 5 min. The yielded PCR products were then electrophoresed on a 1% agarose gel containing ethidium bromide in parallel with 1 Kb Plus DNA Ladder (Invitrogen).

2.4. Phosphoinositide hydrolysis assays

$mGlu_2/H_1$/CHO-K1 cells were plated in 24-well plates at a density of 100,000 cells/well/0.5 mL in growth medium two days before the assay. On the following day, growth media was removed and replace with 0.5 mL/well assay media containing 0.5 μCi/mL [^{3}H]inositol. Cell plates were incubated at 37°C/5% CO_2 overnight and assayed on the third day. For stimulation of phosphoinositide hydrolysis, the [^{3}H] inositol-containing assay medium was first aspirated from wells and replaced with 200 μL of assay buffer (HBSS supplemented with 20 mM HEPES and 30 mM LiCl). Cells were then treated with 250 μL of assay buffer or histamine (2×, 1 μM final concentration, diluted in assay buffer) and 50 μL of serial dilutions of glutamate (10×, diluted in assay buffer). After drug addition, the assay plates were incubated at 37°C/5% CO_2 for 1 h, and then 1 mL of stop solution (10 mM formic acid) was added into each well to terminate the reaction. Cells were incubated in stop solution for 1 h at room temperature then the cell extracts were transferred to anion exchange columns (AG 1-X8 Resin, 100–200 mesh, formate form; Bio-Rad Laboratories, Hercules, CA) for separation of [^{3}H]inositol-containing compounds. After loading of cell extracts, each column was washed sequentially with 9 mL of water, 9 mL of 5 mM inositol, and 9 mL of water. Finally, the [^{3}H]inositol-containing compounds that bound to columns were eluted with 9 mL of PI Eluent (200 mM ammonium formate and 100 mM formic acid) into scintillation vials and measured by liquid scintillation counting. Baseline response was

removed from both histamine-treated and control group respectively and data were fit with GraphPad Prism (La Jolla, CA) to a 4 parameter logistic equation.

2.5. Adenylate cyclase assays

Adenylate cyclase assays were performed according to the methods described in (Watts and Neve, 1996; Sheffler and Conn, 2008). Cells were plated at 60,000 cells/well in Assay Media in 96 well plates 24 h prior to assay. The next day, media was removed from the cells and replaced with 100 μL of serum free DMEM containing 20 mM HEPES. After 1 h incubation at 37 °C, the media was replaced with 50 μL 37 °C stimulation buffer (DMEM, 15 mM HEPES, pH 7.4, 0.025% ascorbic acid). After a 10 min incubation at room temperature, the stimulation buffer was removed and the cells were placed on ice. For dose response curves of glutamate in rat $mGlu_4$/CHO-K1 cells and rat $mGlu_4/H_1$/CHO-K1 cells, 20 μL of the phosphodiesterase inhibitor 3-isobutyl-1-methylxanthine (IBMX) (4×, 500 μM final concentration, diluted in stimulation buffer) was first added to all wells to prevent cAMP breakdown. 20 μL of stimulation buffer was then added, followed by 20 μL of forskolin (4×, 10 μM final concentration, diluted in stimulation buffer) or DMSO-matched vehicle control. Finally, serial dilutions of glutamate (20 μL, 4×, diluted in stimulation buffer) were added to the wells. For histamine fold-shift experiments in $mGlu_4/G_{qi5}$/CHO-DHFR(−) cell line, cells were treated with 20 μL IBMX (4×, 500 μM final concentration, diluted in stimulation Buffer), 20 μL stimulation buffer or histamine (4×, 10 μM final concentration, diluted in stimulation buffer), 20 μL of forskolin (4×, 20 μM final concentration) or vehicle and 20 μL of serial dilutions of glutamate. For histamine fold-shift experiments in $mGlu_4/H_1$/CHO-K1 cells, serial dilutions of $mGlu_4$ PAMs were diluted as 4× stock in stimulation buffer containing 4 μM glutamate (1 μM final concentration). Cells were treated with 20 μL IBMX (4×, 500 μM final concentration, diluted in timulation Buffer), 20 μL of forskolin (4×, 20 μM final concentration) or vehicle, 20 μL stimulation buffer or histamine (4×, 300 nM final concentration, diluted in stimulation buffer) and 20 μL of serial dilutions of $mGlu_4$ PAMs.

After 20 min incubation in water bath at 37 °C, drugs were then removed from the wells and the reaction was terminated by addition of 40 μL ice-cold 3% trichloroacetic acid (TCA). Cell lysates were chilled at 4 °C for at least 2 h. Accumulated cAMP was quantified using a competitive binding assay adapted from (Nordstedt and Fredholm, 1990) with minor modifications. Briefly, TCA extracts (15 μL) from assay plates were added to a deep-well 96 well plate (Axygen Scientific) in triplicates. [^{3}H]cAMP (PerkinElmer) (1 nM final concentration) was diluted in cAMP Assay Buffer (100 mM Tris–HCl, pH 7.4, 100 mM NaCl, 5 mM EDTA) and added to each well (25 μL/well). Lastly, 500 μL of cAMP-binding proteins (approximately 100 μg of crude extract from bovine adrenal cortex) was added to each well. The deep-well plates were incubated on ice for 2 h and harvested with a Brandel cell harvester (Gaithersburg, MD) onto Whatman GF/B filters. Radioactivity bound to filters was quantified by liquid scintillation counting using a PerkinElmer Top Count. The concentration of cAMP in each well was calculated according to a cAMP standard curve ranging from 0.01 to 1000 pM.

2.6. Positive allosteric modulators of $mGlu_4$

Glutamate, histamine and *N*-Phenyl-7-(hydroxyimino)cyclopropa[*b*]chromen-1a-carboxamide (PHCCC) were purchased from Tocris Biosciences (Ellisville, Missouri). Acetylcholine was purchased from Sigma-Aldrich Incorporated (St. Louis, MO). cis-2-[[(3,5-Dichlorophenyl)amino]carbonyl]cyclohexanecarboxylic acid (VU0155041), *N*-(4-(*N*-(2-chlorophenyl)sulfamoyl)phenyl)picolinamide (4PAM2), and 5-methyl-*N*-(4-methylpyrimidin-2-yl)-4-(1*H*-pyrazol-4-yl)thiazol-2-amine (ADX-88178) were synthesized

in-house according to methods in (Niswender et al., 2008; Reynolds, 2008; Engers et al., 2010; Celanire et al., 2011).

3. Results

3.1. Histamine potentiates calcium mobilization, but not cAMP inhibition, downstream of $mGlu_4$ activation

We have long been interested in the identification and characterization of small molecule positive allosteric modulators (PAMs) of $mGlu_4$ for the symptomatic and disease modifying treatment of Parkinson's disease. To characterize compounds, we employ a cell line in which the normally $G_{i/o}$-coupled $mGlu_4$ is co-expressed with the chimeric G protein G_{qi5} to permit induction of a calcium response downstream of $mGlu_4$ activation, a technique that is commonly employed in high throughput screening campaigns for various 7TMRs as it is an easy and cost-effective method to measure compound activity. In addition to identifying small molecule allosteric modulators, we had designed parallel studies to explore the impact of endogenous neurotransmitters and ligands on the modulation of $mGlu_4$ function. In the course of these studies, we discovered that application of the autacoid histamine to $mGlu_4$-expressing cells, prior to application of a concentration of glutamate designed to induce a 20% maximal response, resulted in a strong potentiation of the calcium mobilization signal normally induced by glutamate in $mGlu_4/G_{qi5}$-expressing cells. In these studies, the potentiation effect of histamine highly resembled the effects of synthetic PAMs of $mGlu_4$, such as the prototype PAM N-Phenyl-7-(hydroxyimino)cyclopropa[b]chromen-1a-carboxamide (PHCCC), with one important difference. While both histamine and PHCCC were able to potentiate the effects of an EC_{20} concentration of glutamate (Fig. 1A and B, "Glutamate Add"), unlike PHCCC, histamine induced a weak response when added alone to $mGlu_4/G_{qi5}$ cells (Fig. 1B, "Compound Add"). In our experience using this $mGlu_4/G_{qi5}$ assay, response of compound alone is not common. In Fig. 1C and D, concentration-response curves are shown for the compound response in the absence and presence of an EC_{20} concentration of glutamate. The control PAM PHCCC was inactive when added alone but exhibited a potency of 5.1 ± 0.3 μM when potentiating the response to a low concentration of glutamate. In contrast, histamine generated a concentration-dependent response alone with a potency of 8.3 ± 1.4 μM; in addition, histamine also potentiated the EC_{20} glutamate response (EC_{50} = 1.2 ± 0.1 μM).

Small molecule PAMs of $mGlu_4$ have been shown to potentiate multiple responses downstream of $mGlu_4$ activation (Niswender et al., 2008; Jones et al., 2011). Therefore, if histamine directly binds to the $mGlu_4$ protein and acts as a prototypical $mGlu_4$ PAM, it would be expected to modulate additional, $G_{i/o}$-dependent pathways downstream of $mGlu_4$ activation, such as cAMP inhibition. In contrast to our studies with calcium mobilization (Figs. 1B, 1D and 2A), histamine did not potentiate the ability of $mGlu_4$ activation to inhibit cAMP levels (Fig. 2B). These results suggested that histamine induced biased signaling downstream of $mGlu_4$ activation. It also indicated that the mechanism of histamine's potentiation might differ from previously identified small molecule PAMs.

3.2. Histamine potentiation of glutamate-induced calcium mobilization downstream of $mGlu_4$ requires the presence of the H_1 histamine receptor

While our previous results did not rule out the possibility that histamine directly interacted with $mGlu_4$, the distinct signaling profile induced by histamine suggested that the mechanism of histamine's potentiation might be due to activity at a site distinct from $mGlu_4$, such as a histamine receptor. To determine if low levels of endogenous histamine receptors were involved in mediating the potentiation response, we performed RT-PCR experiments from our $mGlu_4$-expressing cells and determined that they expressed low levels of H_1

histamine receptor mRNA (Fig. 3A). PCR with primers against H_2, H_3 and H_4 receptor did not yield any specific bands to support the existence of other histamine receptors (Supplemental Fig. 1). To address the potential contribution of functional activity of G_q-coupled H_1 receptors, we co-applied the H_1 receptor antagonist mepyramine and 100 μM histamine to $mGlu_4$-expressing cells in the first addition and then added an EC_{20} concentration of glutamate in the second addition. These studies revealed that mepyramine blocked the response induced by histamine application alone to a baseline level (Fig. 3B), consistent with full blockade of H_1. While mepyramine was also able to block the response induced by the glutamate EC_{20} addition, the blockade saturated at the level of the EC_{20} glutamate response (Fig. 3B).

These findings suggested that the potentiation effect was likely mediated by low levels of endogenous H_1 protein present in our $mGlu_4$ cell line. However, they did not completely rule out the possibility of direct histamine binding to $mGlu_4$, since mepyramine might have exerted its effect by displacing binding of histamine from the $mGlu_4$ receptor. Additionally, our original cell line contained the chimeric G protein G_{qi5} to induce $mGlu_4$-mediated calcium mobilization, which would not be reflective of $mGlu_4$ signaling in native tissues. In order to test the hypothesis that the potentiation effect was definitively mediated by H_1 activity versus direct histamine interaction with $mGlu_4$ and occurred in presence of native cellular G proteins, we screened a panel of cell lines to identify a line that did not express H_1 mRNA. We found that CHO-K1 cells, in contrast to the CHO-DHFR(−) cell background used for the initial screening, did not express H_1 mRNA (Fig. 3A). By utilizing the CHO-K1 cells as the parental cell line, we generated two new cell lines that contained either the $mGlu_4$ receptor alone, or $mGlu_4$ co-expressed with the H_1 receptor; neither of these cell lines contained G_{qi5}. As shown in Fig. 4A, $mGlu_4$ was functional and coupled to glutamate-induced cAMP inhibition in cells expressing either $mGlu_4$ alone or the $mGlu_4$ + H_1 combination. We then performed studies in which we attempted to potentiate glutamate-induced calcium mobilization using increasing concentrations of histamine in cells without (Fig. 4B) and with (Fig. 4C) H_1. These results clearly showed that the potentiation required the presence of H_1 receptors.

3.3. The potentiated calcium signal can be generalized to other receptor combinations

According to our findings, the potentiated calcium response that we observed was mediated by concomitant activation of the G_q-coupled H_1 receptor and $G_{i/o}$-coupled $mGlu_4$ receptor. We speculated that, if this potentiation was due to a signaling convergence, the phenomenon would extend to other G_q and $G_{i/o}$-coupled receptor pairs. To test this hypothesis, we co-expressed $mGlu_4$ with the muscarinic acetylcholine M_1 receptor, another G_q-coupled receptor which is also extensively expressed in the CNS. We observed that activation of the M_1 receptor via acetylcholine in this $mGlu_4$-co-expressing cell line induced similar glutamate-dependent calcium mobilization compared to cells co-expressing H_1 and $mGlu_4$ (Fig. 5A). We also hypothesized that such signaling crosstalk might be generalizable to other $G_{i/o}$-coupled mGlu receptors. As carried out for $mGlu_4$, we constructed two $mGlu_2$ cell lines in a CHO-K1 background, one of which expressed $mGlu_2$ alone and the other in combination with H_1 receptor. As shown in Fig. 5B, cells expressing $mGlu_2$ alone did not respond to histamine; in contrast, cells co-expressing H_1 and $mGlu_2$ exhibited robust potentiation of calcium responses after co-application of histamine and glutamate (Fig. 5C). As shown previously (Rives et al., 2009), signaling of $G_{i/o}$ and G_q receptors converges on the PLC_β pathway. To determine if this was also the mechanism of potentiated calcium responses for the receptors examined here, phosphoinositide hydrolysis assays were performed in cells co-expressing $mGlu_2$ and H_1 receptors. Consistent with our observations in calcium mobilization assays, histamine dramatically potentiated $mGlu_2$-induced phosphoinositide hydrolysis (Fig. 5D).

3.4. Co-activation of H_1 and $mGlu_4$ induces functionally selective effects in the presence of multiple $mGlu_4$ positive allosteric modulators

We are very interested in the development of small molecule positive allosteric modulators of $mGlu_4$ and were particularly intrigued with our initial studies (Fig. 2) that suggested that histamine may induce functionally selective activation of signaling pathways downstream of $mGlu_4$. Furthermore, we hypothesized that co-application of histamine with $mGlu_4$ PAMs could further selectively potentiate calcium responses compared to signaling induced by other $G_{i/o}$-dependent pathways. To evaluate this hypothesis, we used our generated $mGlu_4$/H_1/CHO-K1 cell line which does not express G_{qi5}. For these studies, we chose PAMs from four distinct chemical scaffolds (Celanire et al., 2011; Niswender et al., 2008; Reynolds, 2008) (Fig. 6). These compounds were chosen based on differential *in vitro* potency and efficacy at $mGlu_4$; additionally, VU0155041 displays allosteric agonist activity in some assays (Niswender et al., 2008) and has been proposed to bind to a different site on the $mGlu_4$ receptor compared to PHCCC and 4PAM-2 (Drolet et al., 2011). In these experiments, we added increasing concentrations of each PAM either alone or in combination with histamine in the first addition. As shown in Fig. 7, addition of each PAM alone (white traces, “Compound/Histamine Add”) resulted in no calcium mobilization, even after glutamate addition (“Glutamate Add”). Addition of 300 nM histamine alone induced a relatively strong calcium response (dark gray traces); no potentiation of glutamate (second addition) was observed in this case due to the low concentration of glutamate added in these experiments. In contrast, addition of histamine + PHCCC, 4PAM-2, or ADX88178 (Fig. 7A, B, and C) resulted in a prolonged calcium transient after the first addition and a very strong potentiation of the glutamate addition. Consistent with its potential to display allosteric agonist activity in some assays, VU0155041 behaved differently from the other PAMs, and substantial potentiation was observed in the first addition when this compound was added with histamine (Fig. 7D); in contrast, no further potentiation was observed during the glutamate addition. In Fig. 8, the concentration-response curves for these compounds, plus and minus 100 nM and 300 nM histamine, are plotted for the PAM (Fig. 8A, B, and C) and agonist (Fig. 8D) windows of the experiments shown in Fig. 7; the responses to histamine in this assay are clearly concentration-dependent and the potencies of the PAMs obtained are consistent with the potencies observed in other assays (Niswender et al., 2008; Engers et al., 2010; Celanire et al., 2011).

In parallel experiments designed to test the potential for functional selectivity, we assessed the ability of histamine to affect cAMP inhibition responses induced by these PAMs in these same cells. For these studies, we performed concentration-response curves of these compounds, in the presence of an EC_{20} concentration of glutamate, with or without 300 nM histamine. Again, in contrast to calcium mobilization assays and as can be seen in Fig. 9, histamine did not affect the cAMP responses to any of the PAMs tested. These results further suggest that co-activation/potentiation of the histamine H_1 receptor and $mGlu_4$ results in functionally selective effects, resulting in unexpected calcium mobilization induced by $mGlu_4$ PAMs.

4. Discussion

Functional selectivity induced by 7TMR ligands is emerging as an important theme in signaling regulation. As more allosteric modulators are pursued in the hopes of achieving highly selective drug leads with good pharmacokinetic properties, further complexity induced by signal bias will continue to develop. While functional selectivity clearly complicates the use of compounds as general tools for probing receptor function and the progression of drugs with these properties through clinical development, there is great promise in this approach to eventually tailor drug therapy to a particular pathway or subset of signaling cascades to enhance therapeutic efficacy and/or reduce side effects.

In terms of orthosteric ligands, some of the best examples of functional selectivity stem from results with family A 7TMRs, particularly serotonin (5-HT) receptors. For example, orthosteric ligands at the 5-HT_{2A} and 5-HT_{2C} receptors have revealed different rank orders of agonists to stimulate phospholipase C versus phospholipase A2 pathways (Berg et al., 1998). From original models of "linear efficacy", this observation would not have been predicted and called into question the manner in which ligands propagate signals via 7TMRs. There are now examples of ligands with inverse agonist properties in certain pathways but clear agonist activity in others (De Deurwaerdere et al., 2004). Additionally, it has been observed that compounds classified as "antagonists" can induce desensitization, internalization, and downregulation of receptors, a property that might be considered "agonistic" in nature (discussed in (Urban et al., 2007)). In a case where functional selectivity may have therapeutic relevance, the β-adrenergic receptor blocker carvedilol acts as an inverse agonist in cAMP pathways but as an agonist in stimulating β-arrestin-mediated ERK phosphorylation (Wisler et al., 2007); this compound clinically shows advantages over other β-blockers in the treatment of heart failure. This complicated and fascinating pharmacology contributes to the overall phenotype of a given ligand in more complex systems such as native tissues, animals, and people and may certainly impact decision making in the compound discovery, optimization, and characterization processes.

As the search for more selective and "drug-like" 7TMR ligands has grown, the development of allosteric ligands, including PAMs, has emerged. PAMs are an attractive strategy to increase receptor activity as they are predicted to maintain temporal and spatial control of receptor activity and may have advantages versus chronic agonist treatment in terms of receptor desensitization. As these compounds bind to alternate sites on a 7TMR compared to the endogenous ligand, it might be expected that they could place the receptor in a unique structural conformation that might not be achieved, or at least favored, in their absence. This could result in preferential regulation of certain pathways in the presence of an allosteric ligand. For example, the $mGlu_5$ PAM *N*-{4-chloro-2-[(1,3-dioxo-1,3-dihydro-2*H*-isoindol-2-yl) methyl]phenyl}-2-hydroxybenzamide (CPPHA), which binds to an alternate site on the $mGlu_5$ receptor versus other PAMs (O'Brien et al., 2004), exhibits differential effects on calcium mobilization and ERK1/2 phosphorylation downstream of $mGlu_5$ activation in cultured cortical astrocytes (Zhang et al., 2005). This is in contrast to the PAM 3,3′-difluorobenzaldazine (DFB), which potentiates both responses similarly. These results suggest that it is possible for PAMs with distinct *in vitro* properties to exhibit signaling bias, which may translate into different properties in native tissue settings and, possibly, *in vivo*.

In the current manuscript, we have explored the ability of convergent signaling to induce functionally selective effects downstream of allosteric modulation. These studies capitalized on initial reports, such as those of Rives et al. (Rives et al., 2009), showing that convergent signaling downstream of the $G_{i/o}$-coupled $GABA_B$ and G_q-coupled $mGlu_1$ receptors could result in potentiated calcium signaling. The effects reported in Rives et al. were apparent in transfected cells as well as in neurons, indicating that this potentiation can be observed in native tissues. We observed a similar interaction between $mGlu_4$ and H_1 histamine receptors in terms of calcium mobilization. In previous studies (Rives et al., 2009), the mechanism for potentiation was a convergence of signaling via G_q G proteins and the $G_{\beta\gamma}$ subunits of the $G_{i/o}$ G protein at the level of $PLC_{\beta 3}$. To explore the generalizability of this phenomenon for different mGlus, in addition to our $mGlu_4$ and H_1 cells lines, we generated cells expressing $mGlu_4$ and the G_q coupled M_1 muscarinic receptor as well as cells co-expressing $mGlu_2$ and H_1. As shown in Fig. 5, activation of the M_1 receptor via acetylcholine in $mGlu_4$-co-expressing cells induced similar glutamate-dependent calcium mobilization compared to cells co-expressing H_1 and $mGlu_4$. As shown for $mGlu_4$, CHO-K1 cells expressing $mGlu_2$ alone did not respond to histamine; in contrast, cells co-expressing H_1 and $mGlu_2$ exhibited robust potentiation of calcium responses when histamine and glutamate were co-applied.

Finally, consistent with signaling that converges on the PLC_β pathway by co-activated $G_{i/o}$ and G_q receptors (Rives et al., 2009), histamine dramatically potentiated $mGlu_2$-induced phosphoinositide hydrolysis, suggesting that the potentiation mechanism we are observing here is similar. Since PLC_β can be activated by both $G_{\alpha q}$ and $G_{\beta\gamma}$ subunit from the G_i G protein, we propose that occupation of both might have a synergistic effect on IP_3 production, inducing potentiated calcium mobilization. Indeed, mutagenesis studies of the $PLC_{\beta 2}$ protein have shown that distinct binding sites may exist for $G_{\alpha q}$ and $G_{\beta\gamma}$ on the enzyme (Lee et al., 1993).

The present studies extend previous observations by showing that the potentiation effect induced by G_q and $G_{i/o}$ convergent activation is signaling pathway specific and does not extend to other $G_{i/o}$-mediated signaling events, such as cAMP inhibition. These findings suggest that this cascade convergence effectively results in functional selectivity at a signaling level. During the course of our development of $mGlu_4$ PAMs, we have been interested in potential signaling bias or functionally selective effects induced by these compounds, particularly ligands belonging to different chemical scaffolds. In the assays we have examined, the majority of $mGlu_4$ PAMs will potentiate multiple signaling pathways downstream of $mGlu_4$ activation, including calcium mobilization induced using the chimeric G protein G_{qi5} and GIRK channel activation (Niswender et al., 2008; Jones et al., 2011), in addition to potentiation of cAMP inhibition as shown in the present manuscript. Our studies here show that the signal bias induced by histamine can be greatly potentiated in the presence of small molecule PAMs, with PAMs and histamine inducing dramatic potentiation of calcium responses versus other $G_{i/o}$-dependent responses. More importantly, our studies now show that PAMs with no ability to potentiate glutamate-dependent calcium mobilization alone in the absence of chimeric G proteins (Fig. 7, white traces) can induce substantial calcium signaling when the H_1 receptor, and presumably other G_q coupled receptors, are co-activated (Fig. 7, black traces).

This unmasking of a substantial calcium response could be highly important in the physiological effects induced by PAMs *in vivo*. While the H_1 receptor and $mGlu_4$ do exhibit different expression patterns in neurons (for example, $mGlu_4$ is predominantly presynaptic and H_1 predominantly postsynaptic), there are locations where their expression may overlap, such as dendritic cells of the immune system (Fallarino et al., 2010; Vanbervliet et al., 2011). Additionally, the observations that signaling convergence can extend to other receptor pairs suggests that it is highly likely that there are locations in which G_q and $G_{i/o}$ receptors may co-localize. In particular, $mGlu_2$ is expressed in many postsynaptic neurons (Neki et al., 1996; Petralia et al., 1996) and $mGlu_2$ PAMs are currently being developed for schizophrenia treatment, suggesting that a similar phenomenon may also impact $mGlu_2$ PAM signaling in postsynaptic neurons.

Another interesting point of speculation is that the strategy outlined here might provide a viable mechanism to potentiate the signaling of an intractable target. For example, there is substantial evidence indicating that activation of H_1 in neurons may have beneficial effects in terms of attention and wakefulness (reviewed in (Thakkar, 2011)). Due to the substantial expression of H_1 in various immune system cells, however, it would be difficult to pursue direct H_1 agonists or PAMs as drugs for attention without inducing substantial adverse effects. Exploiting the activity of a convergent signaling partner, however, might be an alternate mechanism by which to increase signaling of a G_q coupled 7TMR that is difficult to modulate directly. While $mGlu_4$ expression in dendritic cells of the immune system may preclude it as a strategy to potentiate H_1 signaling, restricted postsynaptic neuronal expression of other $G_{i/o}$-coupled receptors that are not expressed in immune cells could be an interesting strategy to explore.

In conclusion, we have shown that co-activation of $mGlu_4$ and the H_1 histamine receptor induces strong potentiation of calcium mobilization but not traditional $G_{i/o}$ signaling pathways, indicating functional selectivity in signal transduction. These functionally selective effects are observed in the absence of chimeric or promiscuous G proteins and are synergistically potentiated in the presence of small molecule PAMs. Finally, these studies reveal that signaling events induced by PAMs may be "unmasked" in the presence of convergent signaling by G_q coupled receptors, which may lead to complex and unexpected pharmacology. The concept of functional selectivity may be the next frontier in the translation of novel therapeutics into patient populations, and it is anticipated that further exploration of compound pharmacology will certainly aid in the understanding of therapeutic efficacy and adverse effects.

Supplementary Material

Refer to Web version on PubMed Central for supplementary material.

Acknowledgments

The authors thank Drs. Douglas Sheffler, Gregory Digby, and Michael Klein for their review of the manuscript and we thank Drs. Darren Engers and Corey Hopkins for synthesis of compounds used in this manuscript. These studies were supported by NINDS grant NS0483344 and the Michael J. Fox Foundation. Vanderbilt is Specialized Chemistry Center within the Molecular Libraries Probe Centers Network.

Disclosure statement

The authors have received funding from the Michael J. Fox Foundation to develop positive allosteric modulators of $mGlu_4$ for Parkinson's disease.

Abbreviations

mGlu receptor	metabotropic glutamate receptor
CHO	Chinese Hamster Ovary
DHFR(−)	Dihydrofolate Reductase
DMSO	Dimethyl Sulfoxide
GPCR	G-Protein-Coupled Receptor
7TMR	Seven Transmembrane Spanning Receptor
CNS	Central Nervous System

References

Berg KA, Maayani S, Goldfarb J, Scaramellini C, Leff P, Clarke WP. Effector pathway-dependent relative efficacy at serotonin type 2A and 2C receptors: evidence for agonist-directed trafficking of receptor stimulus. Mol. Pharmacol. 1998; 541:94–104. [PubMed: 9658194]

Bridges TM, Lindsley CW. G-protein-coupled receptors: from classical modes of modulation to allosteric mechanisms. ACS Chem. Biol. 2008; 39:530–541. [PubMed: 18652471]

Celanire S, Bolea C, Bruckner S, Liverton N, Charvin D, Hess F, Poli S, Bournique B, Fonsi M, Polsky-Fisher S, Gibson C, Girard F, Browne S, Dilella A, Lis E, Luo B, Le Poul E, Reynolds I, Campo B. Discovery and characterization of novel metabotropic glutamate receptor 4 (mGluR4) allosteric potentiators. Curr. Neuropharmacology. 2011; 9(Suppl. 1):9.

Conn PJ, Christopoulos A, Lindsley CW. Allosteric modulators of GPCRs: a novel approach for the treatment of CNS disorders. Nat. Rev. Drug Discov. 2009; 81:41–54. [PubMed: 19116626]

De Deurwaerdere P, Navailles S, Berg KA, Clarke WP, Spampinato U. Constitutive activity of the serotonin2C receptor inhibits in vivo dopamine release in the rat striatum and nucleus accumbens. J. Neurosci. 2004; 2413:3235–3241. [PubMed: 15056702]

Drolet R, Tugusheva K, Liverton N, Vogel R, Reynolds IJ, Hess FJ, Renger JJ, Kern JT, Celanire S, Tang L, Poli S, Campo B, Bortoli J, D'Addona D. Binding Property Characterization of a Novel $MGlu_4$ Positive Allosteric Modulator. Society for Neuroscience Abstracts. 2011

Engers DW, Gentry PR, Williams R, Bolinger JD, Weaver CD, Menon UN, Conn PJ, Lindsley CW, Niswender CM, Hopkins CR. Synthesis and SAR of novel, 4-(phenylsulfamoyl)phenylacetamide $mGlu_4$ positive allosteric modulators (PAMs) identified by functional high-throughput screening (HTS). Bioorg. Med. Chem. Lett. 2010; 2017:5175–5178. [PubMed: 20667732]

Fallarino F, Volpi C, Fazio F, Notartomaso S, Vacca C, Busceti C, Bicciato S, Battaglia G, Bruno V, Puccetti P, Fioretti MC, Nicoletti F, Grohmann U, Di Marco R. Metabotropic glutamate receptor-4 modulates adaptive immunity and restrains neuroinflammation. Nat. Med. 2010; 168:897–902. [PubMed: 20657581]

Jones CK, Bubser M, Thompson AD, Dickerson JW, Turle-Lorenzo N, Amalric M, Blobaum AL, Bridges TM, Morrison RD, Jadhav S, Engers DW, Italiano K, Bode J, Daniels JS, Lindsley CW, Hopkins CR, Conn PJ, Niswender CM. The $mGlu_4$ positive allosteric modulator VU0364770 produces efficacy alone and in combination with L-DOPA or an adenosine A2A antagonist in preclinical rodent models of Parkinson's disease. J. Pharmacol. Exp. Ther. 2011

Kenakin T. New concepts in drug discovery: collateral efficacy and permissive antagonism. Nat. Rev. Drug Discov. 2005; 411:919–927. [PubMed: 16264435]

Keov P, Sexton PM, Christopoulos A. Allosteric modulation of G protein-coupled receptors: a pharmacological perspective. Neuropharmacology. 2011; 601:24–35. [PubMed: 20637785]

Lee SB, Shin SH, Hepler JR, Gilman AG, Rhee SG. Activation of phospholipase C-beta 2 mutants by G protein alpha q and beta gamma subunits. J. Biol. Chem. 1993; 26834:25952–25957. [PubMed: 8245028]

Marlo JE, Niswender CM, Days EL, Bridges TM, Xiang Y, Rodriguez AL, Shirey JK, Brady AE, Nalywajko T, Luo Q, Austin CA, Williams MB, Kim K, Williams R, Orton D, Brown HA, Lindsley CW, Weaver CD, Conn PJ. Discovery and characterization of novel allosteric potentiators of M1 muscarinic receptors reveals multiple modes of activity. Mol. Pharmacol. 2009; 753:577–588. [PubMed: 19047481]

Mathiesen JM, Ulven T, Martini L, Gerlach LO, Heinemann A, Kostenis E. Identification of indole derivatives exclusively interfering with a G protein-independent signaling pathway of the prostaglandin D2 receptor CRTH2. Mol. Pharmacol. 2005; 682:393–402. [PubMed: 15870392]

Neki A, Ohishi H, Kaneko T, Shigemoto R, Nakanishi S, Mizuno N. Pre- and postsynaptic localization of a metabotropic glutamate receptor, mGluR2, in the rat brain: an immunohistochemical study with a monoclonal antibody. Neurosci. Lett. 1996; 2023:197–200. [PubMed: 8848265]

Niswender CM, Johnson KA, Weaver CD, Jones CK, Xiang Z, Luo Q, Rodriguez AL, Marlo JE, de Paulis T, Thompson AD, Days EL, Nalywajko T, Austin CA, Williams MB, Ayala JE, Williams R, Lindsley CW, Conn PJ. Discovery, characterization, and antiparkinsonian effect of novel positive allosteric modulators of metabotropic glutamate receptor 4. Mol. Pharmacol. 2008; 745:1345–1358. [PubMed: 18664603]

Niswender CM, Johnson KA, Miller NR, Ayala JE, Luo Q, Williams R, Saleh S, Orton D, Weaver CD, Conn PJ. Context-dependent pharmacology exhibited by negative allosteric modulators of metabotropic glutamate receptor 7. Mol. Pharmacol. 2010; 773:459–468. [PubMed: 20026717]

Nordstedt C, Fredholm BB. A modification of a protein-binding method for rapid quantification of cAMP in cell-culture supernatants and body fluid. Anal. Biochem. 1990; 1892:231–234. [PubMed: 2177960]

O'Brien JA, Lemaire W, Wittmann M, Jacobson MA, Ha SN, Wisnoski DD, Lindsley CW, Schaffhauser HJ, Rowe B, Sur C, Duggan ME, Pettibone DJ, Conn PJ, Williams DL Jr. A novel selective allosteric modulator potentiates the activity of native metabotropic glutamate receptor subtype 5 in rat forebrain. J. Pharmacol. Exp. Ther. 2004; 3092:568–577.

Petralia RS, Wang YX, Niedzielski AS, Wenthold RJ. The metabotropic glutamate receptors, mGluR2 and mGluR3, show unique postsynaptic, presynaptic and glial localizations. Neuroscience. 1996; 714:949–976. [PubMed: 8684625]

Pin JP, Comps-Agrar L, Maurel D, Monnier C, Rives ML, Trinquet E, Kniazeff J, Rondard P, Prezeau L. G-protein-coupled receptor oligomers: two or more for what? Lessons from mGlu and GABAB receptors. J. Physiol. 2009; 587(Pt 22):5337–5344. [PubMed: 19723778]

Reynolds, IJ. Novel chemical scaffolds that show activity via intra-cerebroventricularly injection in in vivo antiparkinsonian rodent models. 6th International Meeting on Metabotropic Glutamate Receptors; Taormina, Sicily, Italy. 2008.

Rives ML, Vol C, Fukazawa Y, Tinel N, Trinquet E, Ayoub MA, Shigemoto R, Pin JP, Prezeau L. Crosstalk between GABAB and mGlu1a receptors reveals new insight into GPCR signal integration. EMBO J. 2009; 2815:2195–2208. [PubMed: 19590495]

Sheffler DJ, Conn PJ. Allosteric potentiators of metabotropic glutamate receptor subtype 1a differentially modulate independent signaling pathways in baby hamster kidney cells. Neuropharmacology. 2008; 554:419–427. [PubMed: 18625258]

Thakkar MM. Histamine in the regulation of wakefulness. Sleep Med. Rev. 2011; 151:65–74. [PubMed: 20851648]

Urban JD, Clarke WP, von Zastrow M, Nichols DE, Kobilka B, Weinstein H, Javitch JA, Roth BL, Christopoulos A, Sexton PM, Miller KJ, Spedding M, Mailman RB. Functional selectivity and classical concepts of quantitative pharmacology. J. Pharmacol. Exp. Ther. 2007; 3201:1–13. [PubMed: 16803859]

Vanbervliet B, Akdis M, Vocanson M, Rozieres A, Benetiere J, Rouzaire P, Akdis CA, Nicolas JF, Hennino A. Histamine receptor H1 signaling on dendritic cells plays a key role in the IFN-γ/IL-17 balance in T-cell mediated skin inflammation. J. Allergy Clin. Immunol. 2011; 1244:943–953. [PubMed: 21269673]

Watts VJ, Neve KA. Sensitization of endogenous and recombinant adenylate cyclase by activation of D2 dopamine receptors. Mol. Pharmacol. 1996; 504:966–976. [PubMed: 8863843]

Wisler JW, DeWire SM, Whalen EJ, Violin JD, Drake MT, Ahn S, Shenoy SK, Lefkowitz RJ. A unique mechanism of beta-blocker action: carvedilol stimulates beta-arrestin signaling. Proc. Natl. Acad. Sci. U S A. 2007; 10442:16657–16662. [PubMed: 17925438]

Zhang Y, Rodriguez AL, Conn PJ. Allosteric potentiators of metabotropic glutamate receptor subtype 5 have differential effects on different signaling pathways in cortical astrocytes. J. Pharmacol. Exp. Ther. 2005; 3153:1212–1219. [PubMed: 16135701]

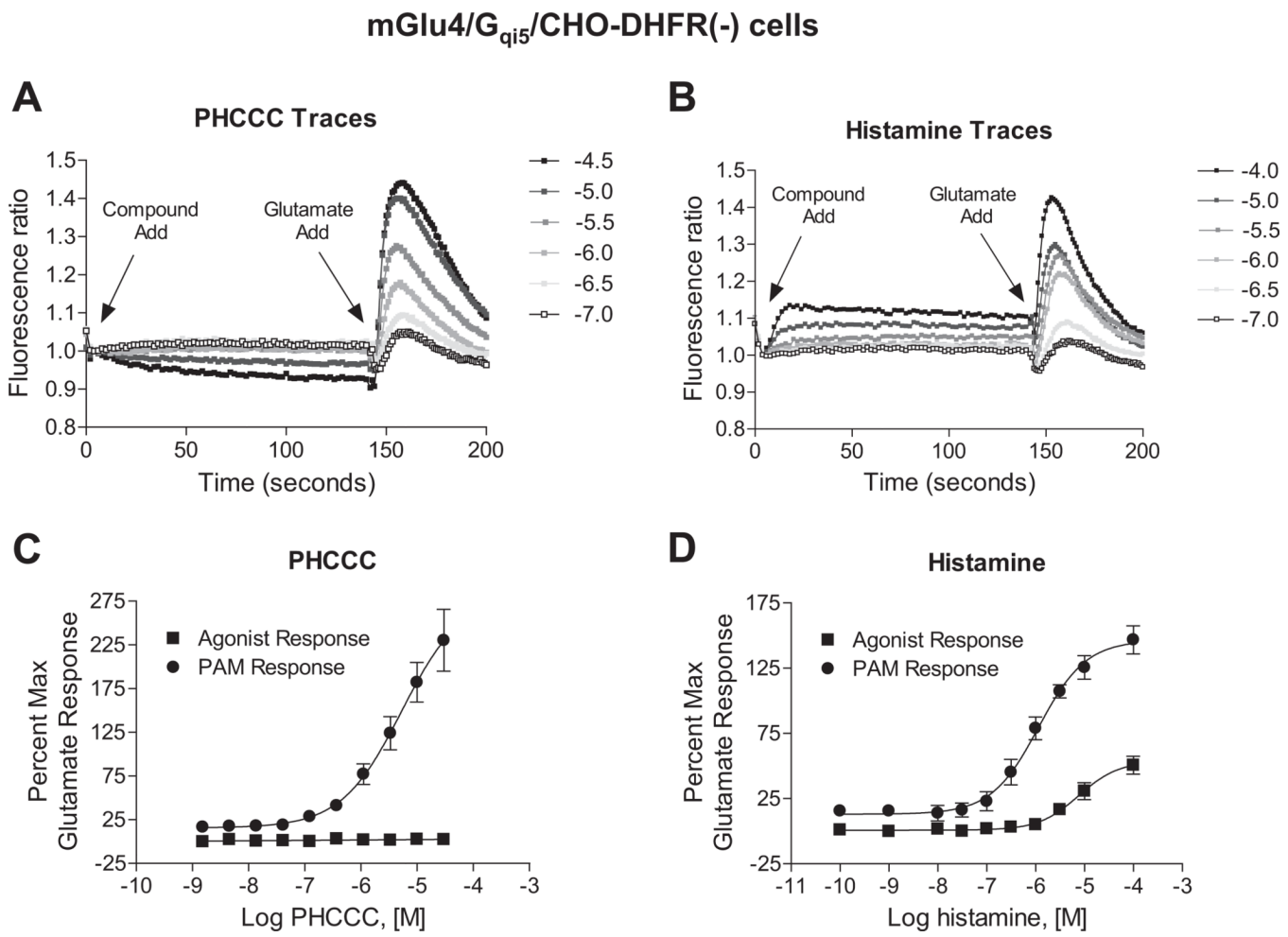

Fig. 1.

Histamine differs from the small molecule $mGlu_4$ PAM, PHCCC, in its potentiation effect. A and B, fluorescence traces of PHCCC and histamine in calcium mobilization assays measured in CHO-DHFR(−) cells co-expressing $mGlu_4$ and the chimeric G protein G_{qi5} in cells. PHCCC (A, ranging from 100 nM to 30 μM) or histamine (B, ranging from 100 nM to 100 μM) was added in the “Compound Add”, while an EC_{20} concentration of glutamate (2.5 μM final) was added after 150 s in the “Glutamate Add”. C and D, Compound activity alone (Agonist Response) and PAM activity (PAM Response) in the presence of an EC_{20} concentration of glutamate (2.5 μM final) from traces represented in A and B are shown for PHCCC and histamine, respectively. For both responses, the increase in fluorescence units is normalized to the maximum response elicited by 1 mM glutamate in this cell line. PHCCC elicited no agonist response and possessed a potency of 5.1 ± 0.3 μM for the PAM response. The potency of histamine for the PAM response was 1.2 ± 0.4 μM and for the agonist response was and 8.3 ± 1.4 μM. Data shown were performed in triplicate; Mean ± SEM.

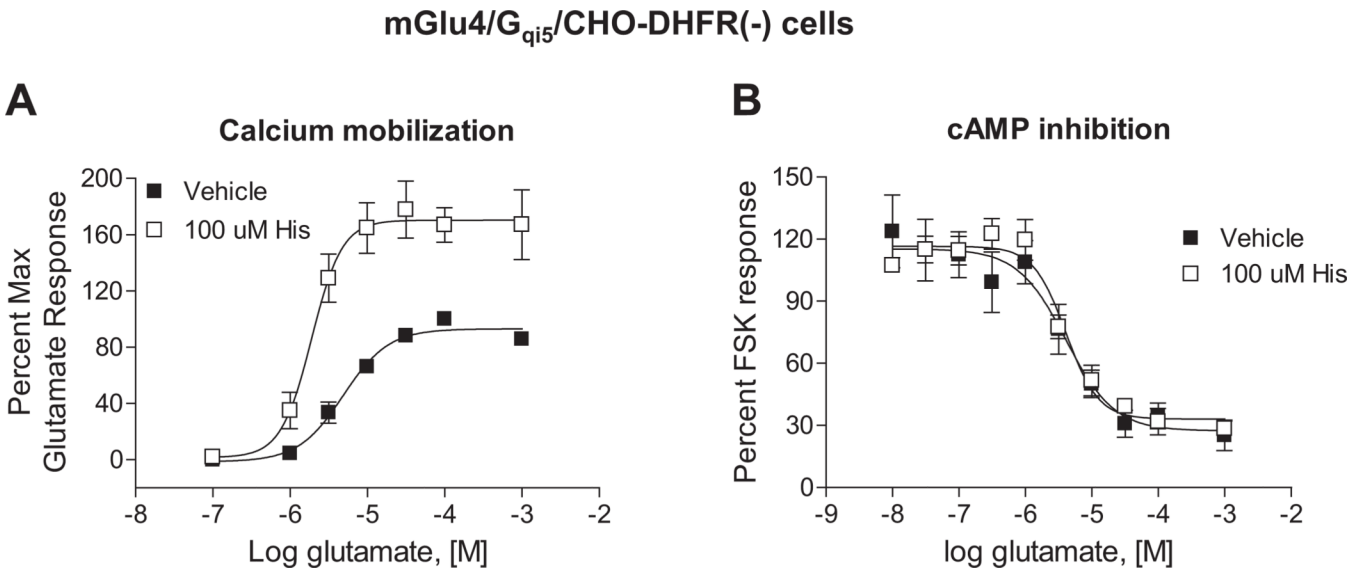

Fig. 2.

Histamine potentiates calcium responses downstream of $mGlu_4$ without impacting glutamate-dependent cAMP inhibition. A, Glutamate-induced calcium mobilization was measured in the presence of vehicle control (■) or 100 μM histamine (□). The responses are normalized to maximum effect of glutamate in the same cell line. Potencies in the absence or presence of 100 μM histamine were 5.1 ± 0.9 μM vs. 2.0 ± 0.3 μM (**p* = 0.029; unpaired *t*-test). Maximal responses in the absence or presence of 100 μM histamine were: 100.0 ± 1.0% vs. 179.1 ± 20.0% (**p* = 0.017; unpaired *t*-test). B, Glutamate-dependent intracellular cAMP concentration was quantified in the absence (■) or presence (□) of 100 μM histamine using a competitive binding assay as described in 2.5. Adenylate cyclase assays. Data were normalized to the 20 μM forskolin-induced response. Potencies in the absence or presence of 100 μM histamine were 4.1 ± 0.3 μM vs. 4.3 ± 0.8 μM (*p* = 0.76; unpaired *t*-test). Maximal inhibition values in the absence or presence of 100 μM histamine were: 88.1 ± 8.3% vs. 83.9 ± 2.3% (*p* = 0.65; unpaired *t*-test). Data shown were performed in triplicate; Mean ± SEM. Statistical analysis was performed using GraphPad Prism (La Jolla, CA).

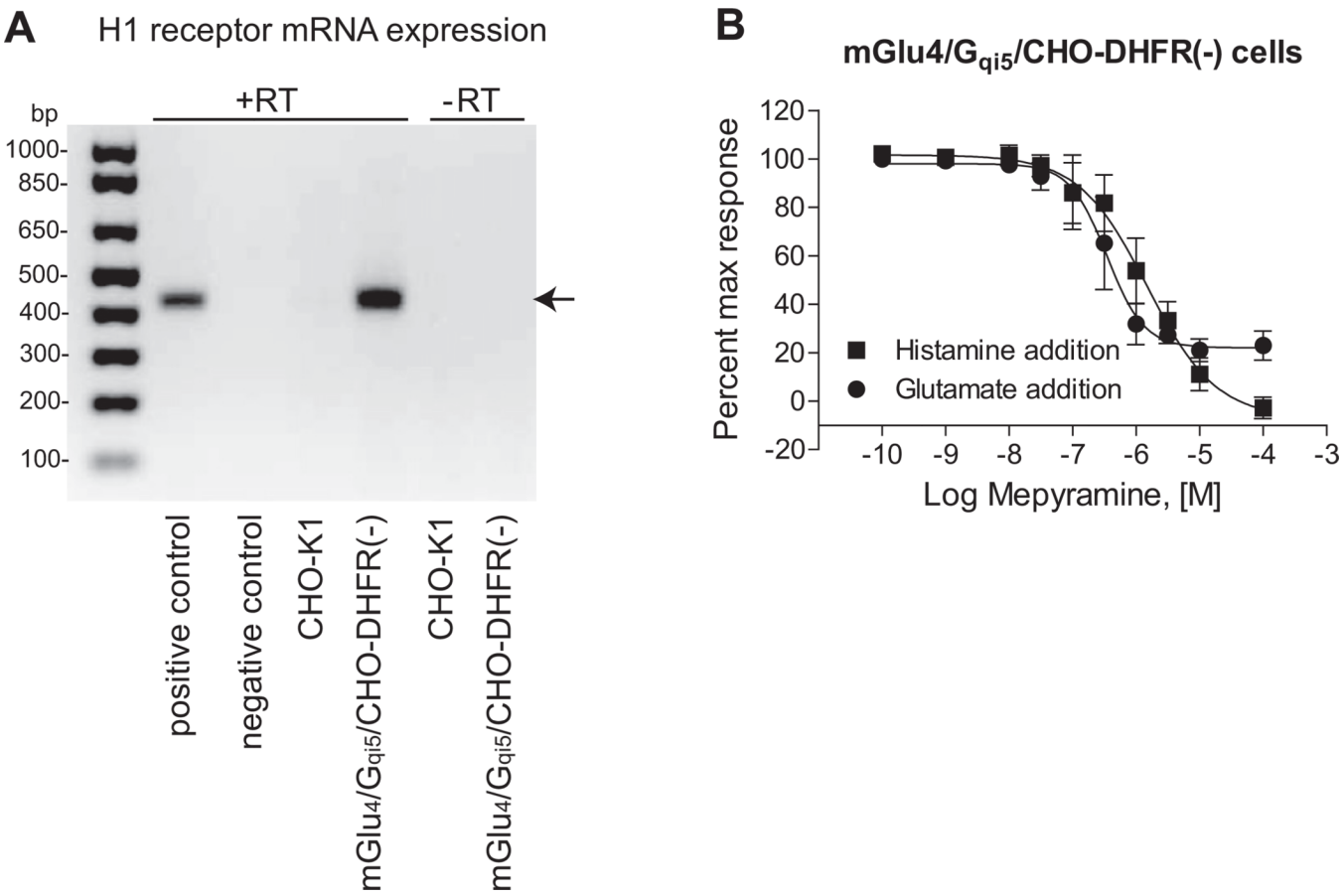

Fig. 3.

The histamine H_1 receptor may be involved in the potentiation effect of histamine. A, mRNA expression of histamine H_1 receptor in different cell lines. mRNA was extracted from CHO-K1 cell line and $mGlu_4/G_{qi5}$/CHO-DHFR(−) cell line and RT-PCR was performed as described under Materials and Methods. "+RT" indicates presence of reverse transcriptase during the reaction of reverse transcription, whereas "−RT" represents absence of reverse transcriptase as negative controls. Predicted size of the PCR product for the H_1 receptor was 423 bp, as shown with arrow. B, Mepyramine abolishes the agonist response and potentiation effect of histamine. Increasing concentrations of mepyramine were added to $mGlu_4/G_{qi5}$/CHO-DHFR(−) cells with 100 μM histamine prior to addition of an EC_{20} concentration of glutamate (2.5 μM glutamate final). Calcium mobilization induced by the histamine addition and the subsequent glutamate addition was measured as described. Potencies of mepyramine in the histamine add or the glutamate add were: 1.55 ± 0.5 μM vs. 393 ± 154 nM ($p = 0.10$; unpaired t-test). Data shown were performed in triplicate; Mean ± SEM. Statistical analysis was performed using GraphPad Prism (La Jolla, CA).

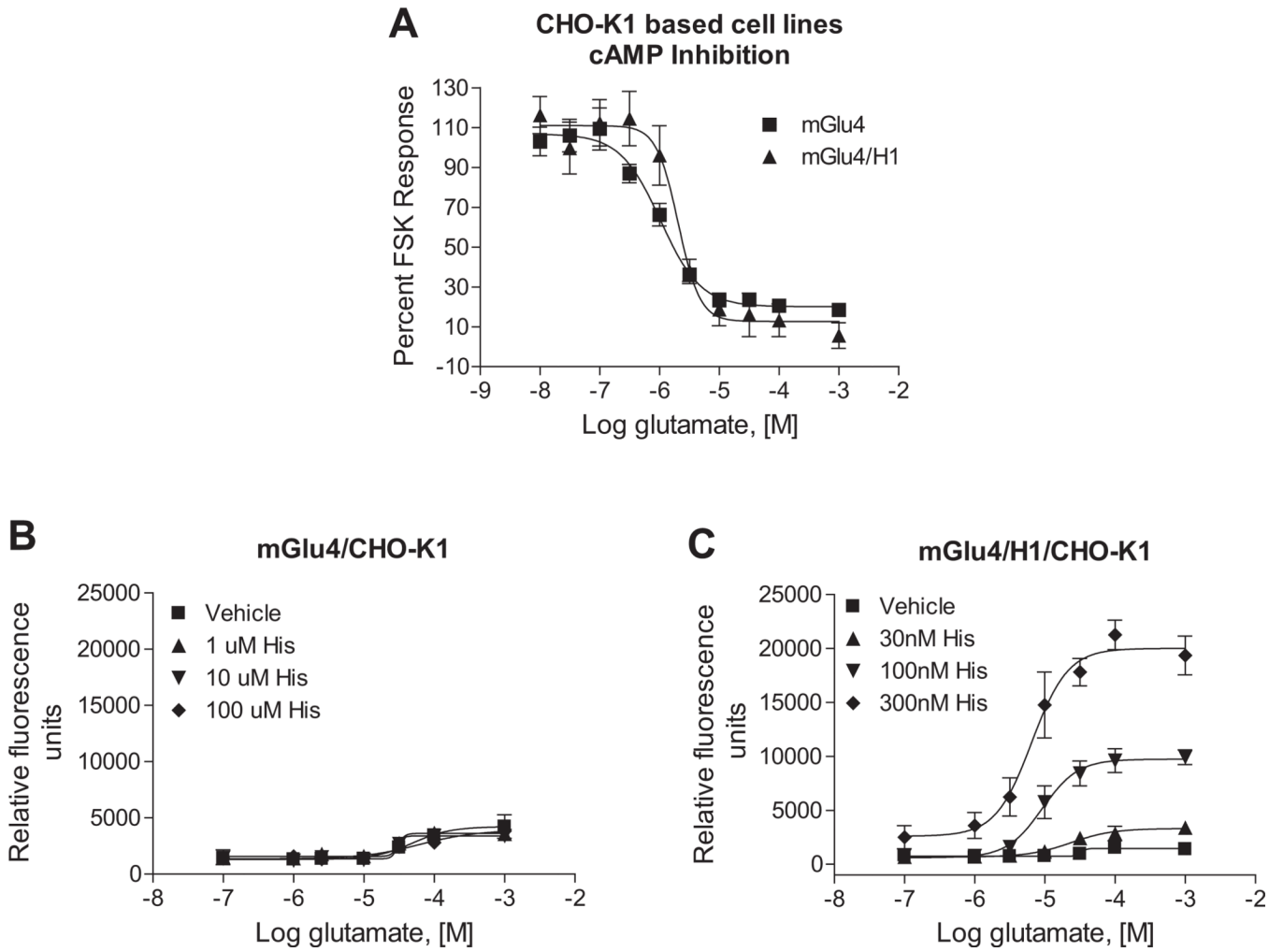

Fig. 4.

The histamine H_1 receptor is required for the potentiation effect of histamine. A, Glutamate exhibits potencies of 1.0 ± 0.03 μM and 2.3 ± 0.1 μM, respectively, in adenylate cyclase assays in $mGlu_4$/CHO-K1 cells and $mGlu_4/H_1$/CHO-K1 cells (*$p = 0.0048$, unpaired *t*-test). Intracellular cAMP concentration was measured as described in 2.5. Adenylate cyclase assays and responses were normalized to the 10 μM forskolin response in each cell line, respectively. B, The effect of 1 μM (▲), 10 μM (▼) and 100 mM (◆) histamine on glutamate-induced calcium mobilization in $mGlu_4$/CHO-K1 cells is shown. Maximal responses of vehicle, 1 μM, 10 μM or 100 μM histamine-treated cells were 3391 ± 1033, 3254 ± 841, 3067 ± 527 and 3214 ± 643 relative fluorescence units, respectively ($p = 0.99$; One-way ANOVA). C, The effect of 30 nM (▲), 100 nM (▼) and 300 nM (◆) histamine in potentiating calcium responses mediated by glutamate in $mGluR_4/H_1$/CHO-K1 cells is shown. Maximal responses in vehicle, 30 nM, 100 nM or 300 nM histamine-treated cells were 1548 ± 230, 3390 μ 636, 10099 μ 819, 21261 μ 1356 relative fluorescence units, respectively (*$p < 0.0001$; One-way ANOVA). Data shown were performed in triplicate; Mean ± SEM. Statistical analysis was performed using GraphPad Prism (La Jolla, CA).

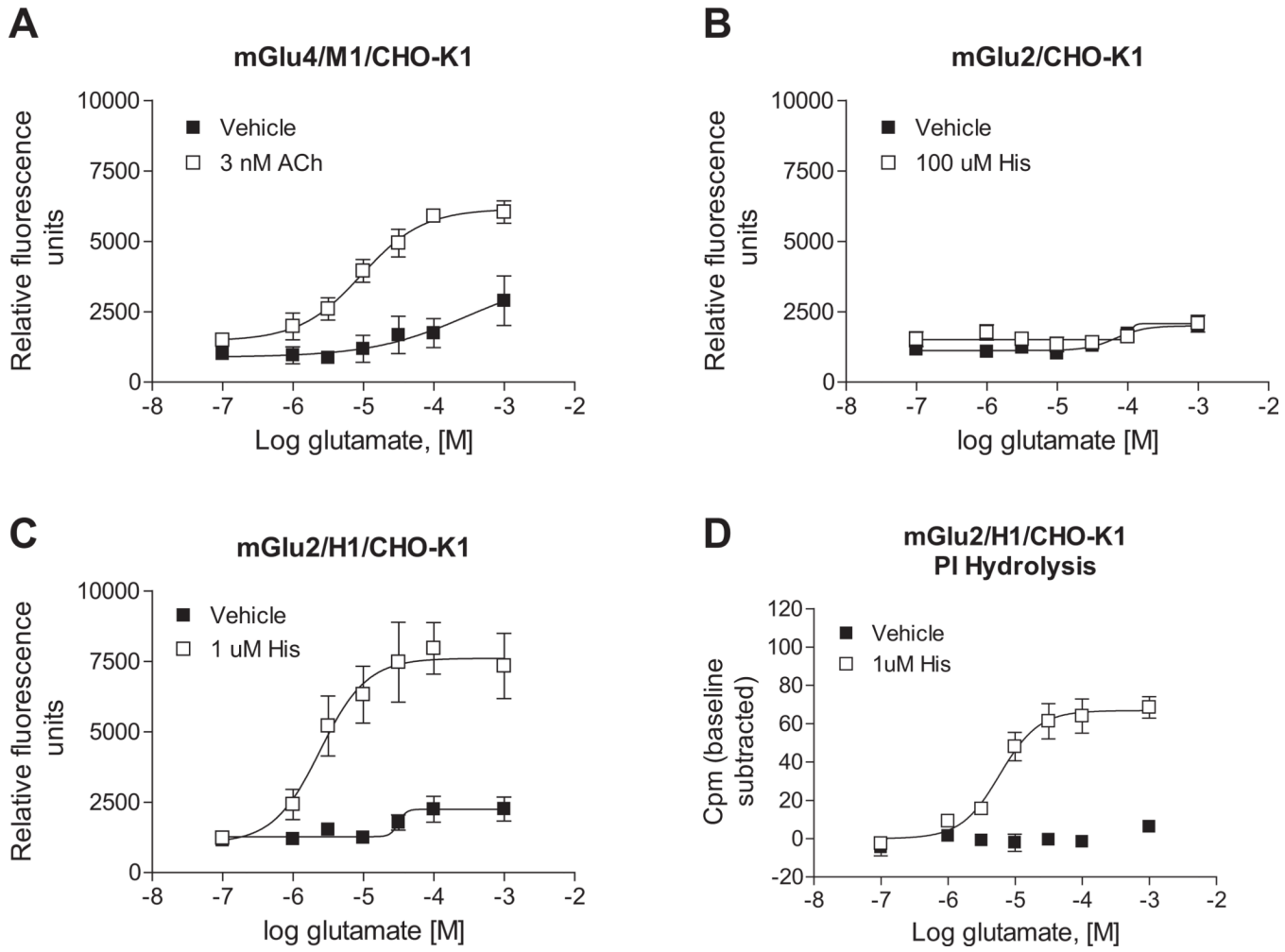

Fig. 5.

Phospholipase C pathway potentiation extends to additional G_q and $G_{i/o}$ pairs. A, Acetylcholine (Ach) potentiates calcium responses induced by $mGlu_4$ activation in $mGlu_4/M_1$/CHO-K1 cells. 3 nM Ach (□) or vehicle (■) control was added to cells in the first add, while increasing concentrations of glutamate were applied 150 s later in the second add and calcium mobilization was measured. Maximal responses in the absence or presence of 3 nM Ach were: 2889 ± 878 vs. 6175 ± 280 relative fluorescence units (*$p = 0.024$; unpaired *t*-test). Data shown were performed in triplicate; Mean ± SEM. B and C, histamine potentiates the calcium response of $mGlu_2$ in the presence of the histamine H_1 receptor in $mGlu_2/H_1$/CHO-K1 cells. In $mGlu_2$/CHO-K1 cells, maximal responses in the absence or presence of 100 μM histamine were: 2072 ± 23.7 vs. 2122 ± 272 relative fluorescence units ($p = 0.86$; unpaired *t*-test). In $mGlu_2/H_1$/CHO-K1 cells, maximal responses in the absence or presence of 1 μM histamine were: 2796 ± 285 vs. 8223 ± 1128 relative fluorescence units (*$p = 0.010$; unpaired *t*-test). Data shown were performed in triplicate; Mean ± SEM. D, Histamine potentiates $mGlu_2$ responses in phosphoinositide hydrolysis assays in $mGlu_2/H_1$/CHO-K1 cells. Cells were treated with increasing concentrations of glutamate in the presence of 1 μM histamine (□) or vehicle control (■). After 1 h incubation at 37 °C, accumulated inositol phosphates were measured according to description in 2.4. Phosphoinositide hydrolysis assays. Maximal responses in the absence or presence of 1 μM histamine were: 6.9 ± 1.8 vs. 68.7 ± 5.8 cpm (*$p = 0.0005$; unpaired *t*-test). Data from

triplicate experiments are shown (Mean ± SEM) with relative baseline responses subtracted from each group. All Statistical analysis was performed using GraphPad Prism (La Jolla, CA).

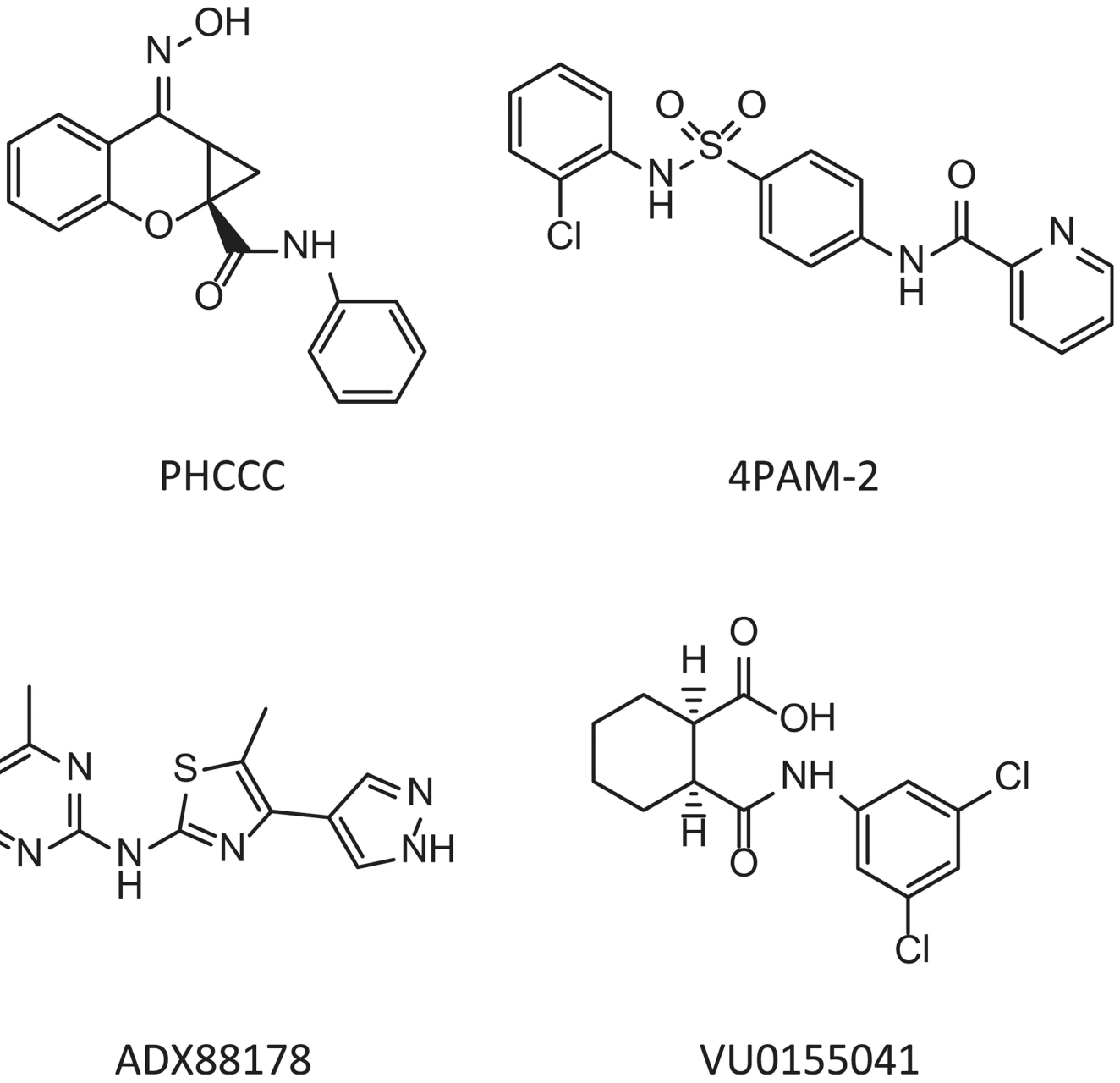

Fig. 6.
Chemical structures of $mGlu_4$ PAMs used in these studies: PHCCC, 4PAM-2, ADX88178 and VU0155041.

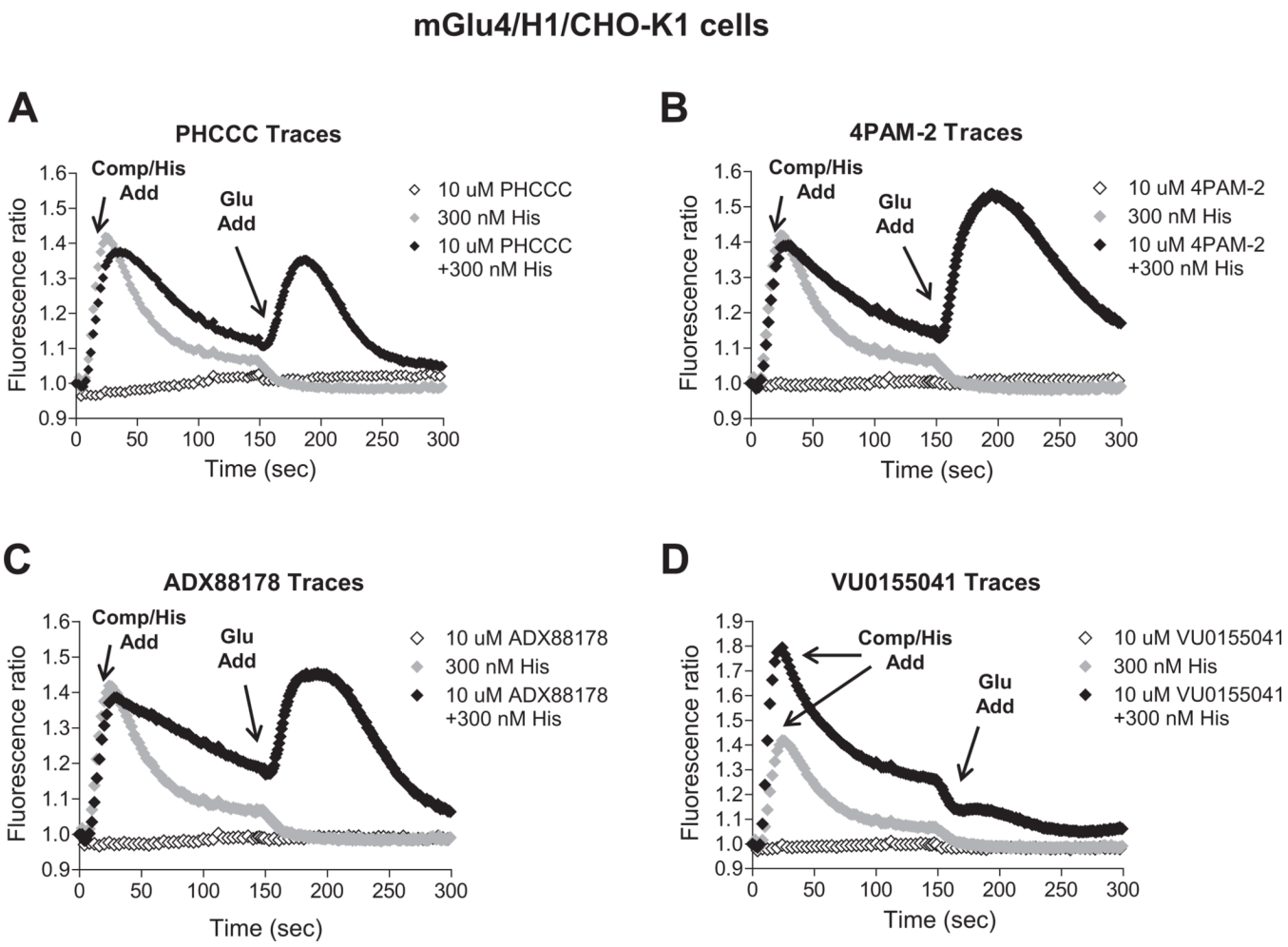

Fig. 7.

Histamine dramatically potentiates the effect of PAMs on $mGlu_4$-mediated calcium mobilization in cells co-expressing $mGlu_4$ and H_1 receptors. Traces of calcium transients showing the effects of $mGlu_4$ PAMs, histamine or the combination of both in potentiating the response of an EC_{20} concentration of glutamate (1 μM glutamate final) are shown. In these traces, a 10 μM concentration of each $mGlu_4$ PAM (PHCCC, 4PAM-2, ADX88178 or VU0155041, in A-D respectively; (◇)), 300 nM histamine (♦) or combination of both (◆) were applied in the first add ("Compound/Histamine Add"). After 150 s, 1 μM glutamate (concentration determined based on cAMP experiments shown in Fig. 4A) was applied in the second add ("Glutamate Add"). Calcium responses were measured as the fluorescence ratio, which involves dividing all fluorescence data for each point in the kinetic trace by the fluorescence value obtained in the first baseline sample read, which corrects for differences in dye loading and cell plating.

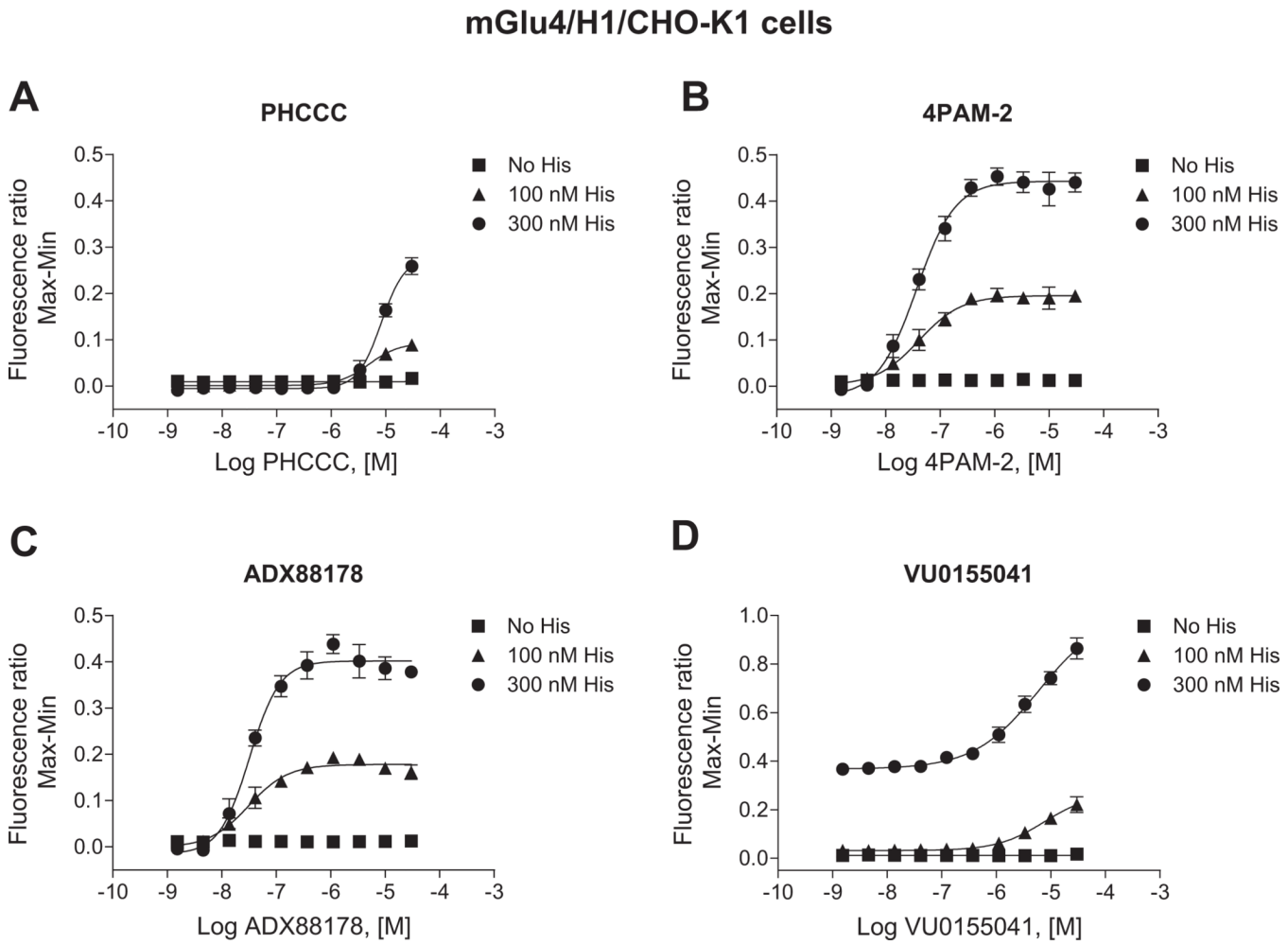

Fig. 8.

Histamine dose-dependently potentiates the efficacy of PAMs on $mGlu_4$-mediated calcium mobilization in cells co-expressing $mGlu_4$ and H_1 receptors. Results of traces in Fig. 7 were plotted in concentration-response curve format. Increasing concentrations of the $mGlu_4$ PAMs PHCCC, 4PAM-2, ADX88178 or VU0155041 (A-D, respectively) were applied either alone (■) or together with 100 nM (▲) or 300 nM (●) histamine in the first add. After 150 s, a 1 μM glutamate concentration was applied in the second add. Calcium responses were measured as the fluorescence ratio, which involves dividing all fluorescence data for each point in the kinetic trace by the fluorescence value obtained in the first baseline sample read, which corrects for differences in dye loading and cell plating. Data were further normalized by taking the maximum calcium response minus the minimum response measured 3 s prior to either the first or second addition. For PHCCC (A), 4PAM-2 (B), and ADX88178 (C) responses, the effect on the second addition ("Glutamate Add") window is shown. For VU0155041 (D), the effect on the first addition ("Compound Add") is shown. Potencies for the different conditions were: PHCCC alone, no fit, PHCCC + 100 nM histamine, 8.2 ± 5.1 μM, PHCCC + 300 nM histamine, 7.6 ± 1.4 μM; 4PAM-2 alone, no fit, 4PAM-2 + 100 nM histamine, 54.2 ± 29.0 nM, 4PAM-2 + 300 nM histamine, 40.8 ± 10.0 nM; ADX88178 alone, no fit, ADX88178 + 100 nM histamine, 37.2 ± 15.1 nM, ADX88178 + 300 nM histamine, 30.0 ± 5.2 nM; VU0155041 alone, no fit, VU0155041 + 100 nM histamine, 9.5 ± 3.9 μM, VU0155041 + 300 nM histamine, 6.5 ± 1.6 μM. Maximal responses in the absence or presence of 100 nM or 300 nM histamine were: for PHCCC,

0.016 ± 0.003, 0.089 ± 0.010, 0.259 ± 0.018 (*$p < 0.0001$; One-way ANOVA); for 4PAM-2, 0.017 ± 0.002, 0.212 ± 0.013, 0.460 ± 0.022 (*$p < 0.0001$; One-way ANOVA); for ADX88178, 0.016 ± 0.002, 0.197 ± 0.003, 0.438 ± 0.020 (*$p < 0.0001$; One-way ANOVA); and for VU0155041, 0.018 ± 0.003, 0.221 ± 0.032, 0.864 ± 0.043 (*$p < 0.0001$; One-way ANOVA). Data shown were performed in triplicate; Mean ± SEM. Statistical analysis was performed using GraphPad Prism (La Jolla, CA).

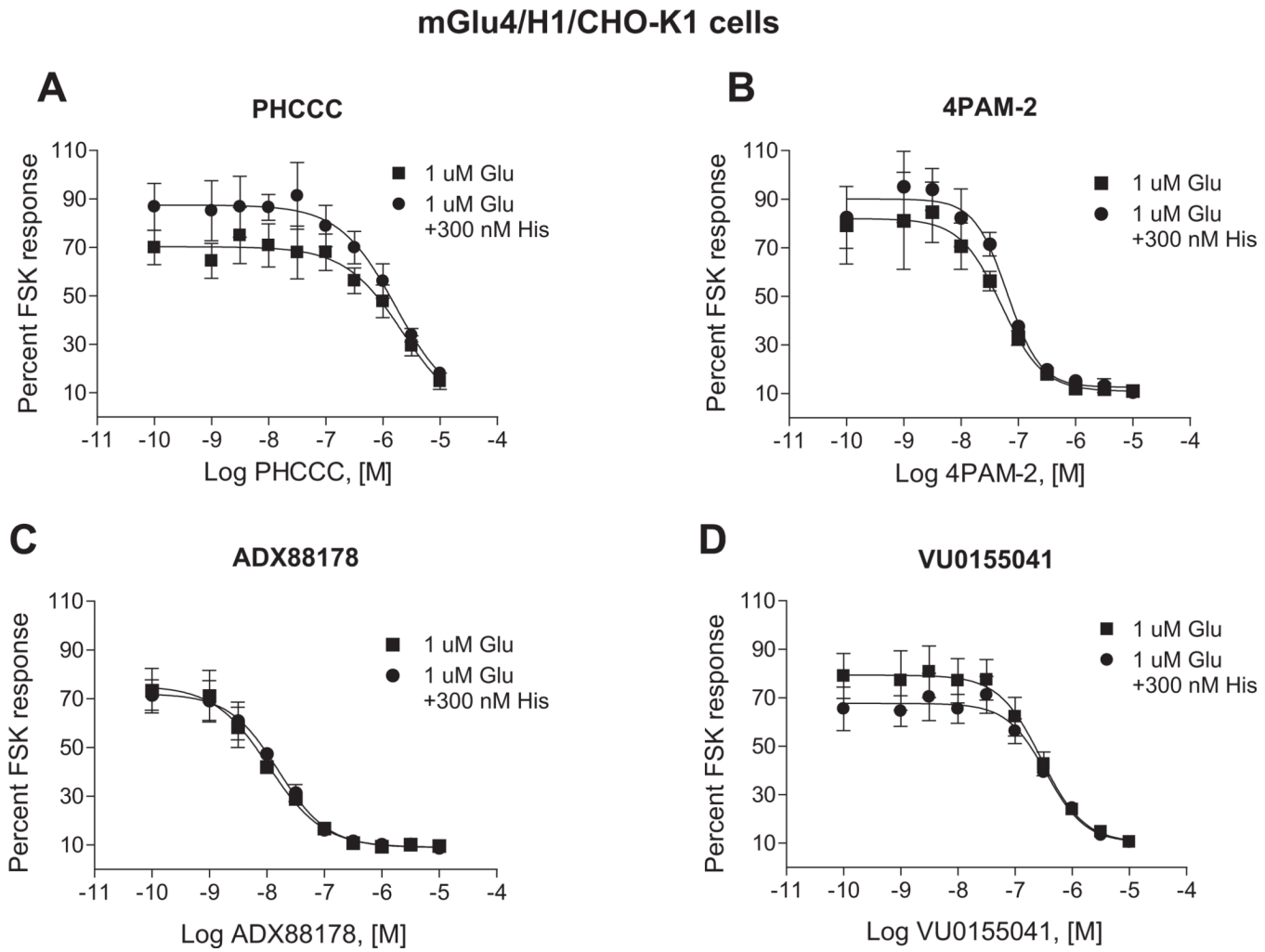

Fig. 9.

In contrast to effects on calcium mobilization, histamine has no effect on the activity of mGlu4 PAMs in adenylate cyclase assays in cells expressing both $mGlu_4$ and H_1 receptors. Increasing concentration of $mGlu_4$ PAMs (PHCCC, 4PAM-2, ADX88178 or VU0155041, A-D, respectively) were co-diluted with 1 μM glutamate and incubated with $mGlu_4/H_1$/CHO-K1 cells either alone or together with 300 nM histamine. Intracellular cAMP concentration was measured as described and then normalized to either 20 μM forskolin response or 20 μM forskolin + 300 nM histamine, respectively. Potencies in the absence or presence of 300 nM histamine were: PHCCC, 2.5 ± 0.6 μM vs. 1.8 ± 0.4 μM ($p = 0.40$; unpaired *t*-test); 4PAM-2, 55.5 ± 12.6 nM v.s 66.1 ± 8.6 nM ($p = 0.53$; unpaired *t*-test); ADX88178, 11.7 ± 2.0 nM vs. 16.0 ± 4.3 nM ($p = 0.42$; unpaired *t*-test); and VU0155041, 287.3 ± 23.1 nM vs. 360.0 ± 38.8 nM ($p = 0.18$; unpaired *t*-test). Maximal inhibition values in the absence or presence of 300 nM histamine were: PHCCC, 85.3 ± 3.4% vs. 82.0 ± 2.7% ($p = 0.49$; unpaired *t*-test); 4PAM-2, 89.0 ± 1.2 nM vs. 89.4 ± 0.6% ($p = 0.77$; unpaired *t*-test); ADX88178, 90.4 ± 1.5% vs. 91.1 ± 0.6% ($p = 0.70$; unpaired *t*-test); and VU0155041, 89.5 ± 0.4% vs. 90.0 ± 0.1% ($p = 0.85$; unpaired *t*-test). Data shown were performed in triplicate; Mean ± SEM. Statistical analysis was performed using GraphPad Prism (La Jolla, CA).